V. A. Ferraresi

Universidade Federal de Uberlândia
Campus Santa Mônica
38400-902 Uberlândia, MG. Brazil
valtairf@mecanica.ufu.br

K. M. Figueiredo

Universidade de São Paulo – USP
Escola de Engenharia de São Carlos
Av. Trabalhador Sancarlense, 400, Centro
13560-970 São Carlos, SP. Brazil

T. Hiap Ong

Universidade Federal de Uberlândia
Campus Santa Mônica
38400-902 Uberlândia, MG. Brazil

Metal Transfer in the Aluminum Gas Metal Arc Welding

Among the aluminum welding processes, the GMAW (Gas Metal Arc Welding) process can be easily made automatic, has high productivity and great versatility regarding the type and thickness of material used in welding. The possibility of changing the transfer mode to adapt to different thickness, joint types, among other aspects, is another important and attractive feature. However, little is known about the transfer modes in aluminum GMAW process. For this reason, in this study an analysis of the metal transfer modes in the aluminum welding was made, and the objective was to generate maps that could identify the metal transfer modes and their regions in relation to the shielding gas and the wire diameter. The experimental procedure was the execution of weld on aluminum plate in a flat position with a constant voltage power source. The methodology used was laser Shadowgraphy combined with a high-speed movie camera. Therefore, it was possible to design the maps in which four metal transfer modes and their respective transition zones were determined. The maps also permit determination of the transition current zone between the globular and the spray mode, and modeling of the melting rate.
Keywords: Aluminum, GMAW process, metal transfer, transition current, melting rate

Introduction

Among the aluminum welding processes, the automated GMAW process has high productivity and great versatility regarding the material type and thickness in welding. However, this process exhibits a few difficulties, such as: higher sensibility to welding parameters variation demanding a rigorous regulation of these parameters in order to obtain an excellent quality of the weld bead (AWS, 1991).

The mode that the droplet is transferred from the wire to the melting pool (known as metal transfer modes) is important in the GMAW process, since it determines the process stability and consequently the quality of the weld fillet (Norrish & Richardson, 1988). In a simple way, the current literature acknowledges three basic forms of metal transfer: short circuit, globular, and spray (AWS, 1991).

The short circuit metal transfer occurs in low voltage values and moderate welding current, and it is characterized by periodic contact of the drop with the melting pool, causing important instability in the welding voltage and current; this may present intense formation of spatters.

The globular metal transfer occurs with intermediary values of current and elevated welding voltage. During welding, the melting metal globule at the tip of the wire grows as time passes, until it detaches under the effect of gravity. This causes a deposition of large drops, much larger than the wire diameter, in the melting pool, occurring spatters.

The spray transfer mode occurs with high voltage and current, above a stripe named transition current (current stripe between globular and spray mode). The drops are small, close to the wire diameter size, which are thrown in high frequency into the melting pool. This mode presents good process stability, and a good aspect of the weld bead with very few spatters ((Norrish & Richardson, 1988 and AWS, 1991).

The knowledge of the transition current zone between the globular and spray mode has great importance in the GMAW process, because it determines the working conditions of the process. The globular mode has limited applications, since it can cause lack of fusion, insufficient penetration, excessive reinforcement, and high amount of spatter in the weld bead (Norrish & Richardson, 1988). On the other hand, the spray mode generates excellent quality and high deposition rate at the weld bead, but it needs high welding energy (high current), and its application is indicated for thick plates. Another relevant factor in the knowledge of the transition current zone is its utilization in pulsed arc transfer, also known as controlled transfer (AWS, 1991).

An important factor in welding is the relation between the wire consumption (melting rate) and the welding current because, with the desired wire consumption together with the joint geometry, the necessary amount of steps to fill the joint can be calculated. Thus, predicting the work current and, consequently, the wire feed speed, will help the source adjustment. Experimentally, the principal factors that influence the wire consumption are the generated heat in the wire, through the Joule effect, and its wire-arc connection (cathodic region) (Quites & Dutra, 1979). Lesnewich (1958) proposes the equation below for the melting rate (MR).

$$MR = \boldsymbol{a}.I + \boldsymbol{b}.l.I^2 \qquad (1).$$

In which l is the wire length, I is the current, and the constant $\boldsymbol{a}$ characterizes the reactions that occur in the wire-arc connection in function of the shielding gas type, wire type, and current polarity. As for the constant $\boldsymbol{b}$, it is related to wire voltage drop, representing the Joule effect and is, therefore, influenced by the wire characteristics, i.e., by the diameter, length, and material. The α and β constants are determined experimentally.

The aim of this paper is to map the metal transfer modes in aluminum GMAW welding, varying the shielding gas type and the wire diameter. Furthermore, the globular/spray transition current range and the α and β constants of the consumption equation were determined to verify the influence of the welding parameters (shielding gas and wire diameter) on consumption and transition current.

Experimental Procedure

The welding were carried out in a flat position with the electronic source in constant voltage mode. Experiments with the variation of reference voltage and the wire feed speed (consequently

the current) were carried out. The 15 l/min gas flux, the 15 mm contact tip to work distance, and the 10^0 torch slope in the forehand technique were maintained constant.

The test specimens were made from aluminum plate of AA 5052 (Al-Mg alloy) and ¼" (6.35 mm) thick. AWS ER-4043 (Al-Si alloy) wires with 1.0 mm and 1.2 mm diameter were used as filler metal. For the 1.0 mm diameter wire, tests were made using pure argon (Ar) gas and a mixture of argon (Ar) with 25% of helium (He), and for the 1.2 mm wire, only pure argon gas was used.

A laser Shadowgraphy combined with a high speed movie camera (2000 frames/s) system was utilized to determine the diameter, frequency, and the transfer mode of the drops (Figueiredo & Ferraresi, 2000). During welding, current and voltage acquisition was also carried out.

Results And Discussions

The experiments accomplished and their results are presented in Tables 1, 2, and 3, where: N^O is experiment number; WS is wire feed speed; TS is travel speed; I_a is average current; U_{ref} is reference voltage; U_a is average voltage; l is wire length; SD is standard deviation; D_{drop} is average drop diameter; F is droplet deposition frequency; Modtrans is metal transfer mode; SC is short circuit; GL is globular; SP is spray; GL/SC is globular/short circuit; and # indicates that in this test transfers, with combined modes, occurred in a random mode, i.e, they were not stable and there was an interchanging random combination among the transfer modes.

Through analysis of the images and the voltage and current values acquired during the welding, it was possible to detect 4 (four) metal transfer modes, also indicated in the tables: Short Circuit (SC), Globular (GL), Spray (SP), and Globular/Short Circuit (GL/SC).

In the short circuit transfer mode, a high instability of the metal transfer was verified, and most of the time, a drop repulsion before the final transfer, was observed, causing high oscillations in the welding current and voltage. Figure 1 shows a photo sequence of this transfer mode showing the drop repulsion at the moment of transfer. The time lapse between frames is 0.5ms (for example, the time lapse between SC080 and SC090 is 5ms).

According to literature (Norrish & Richardson, 1988; AWS, 1991), in the globular transfer mode, the drop diameter is larger than the wire diameter. Because a minimum size of the drop is not specified to determine the transition between the globular and spray mode, and based on the observation of the metal transfer recorded, it was accepted that the globular mode occurs with drops having average diameter 15% above the wire diameter. Therefore, the drops with average diameter smaller than this values were considered as spray transfer mode. In spray transfer mode, drops with average diameter smaller than the wire diameter were not obtained. Figure 2 shows the sequence of photos of globular transfer and Figure 3 that of spray transfer.

Scotti et. al. (1999) explained that in globular/short circuit transfer mode, the drop has globular formation, and that it ends its transfer with short circuit. This behavior was also observed in the present study. After an exaggerated growth of the drop, which causes its contact with the melting pool and, thus, it transfers to the weld pool. Figure 4 shows a sequence of photos with this transfer mode.

Table 1. Results of the tests with argon gas and 1.0 mm diameter wire.

N^O	WS [m/min]	TS [cm/min]	I_a [A]	U_{ref} [V]	U_a [V]	l [mm]	SD	D_{drop} [mm]	SD	F [Hz]	Modtrans
1	7	32.0	69	16	15.96	12.160	0.626	2.16	0.38	16	GL/SC
2	9	41.1	114	16	15.84	13.393	0.502	1.59	0.19	56	GL/SC
3	11	50.3	141	16	15.98	13.805	0.322	1.39	0.16	129	SC
4	7	32.0	93	18	17.70	11.937	0.745	2.12	0.18	21	GL/SC
5	9	41.1	125	18	17.51	13.097	0.409	1.60	0.13	43	GL/SC
6	11	50.3	126	18	17.97	13.444	0.392	1.70	0.18	50	SC
7	8	36.6	117	20	19.32	12.195	0.530	1.59	0.18	62	#
8	12	54.8	169	20	19.01	13.568	0.322	1.07	0.20	196	SC
9	14	64.0	182	20	18.97	13.869	0.338	1.21	0.12	154	SC
10	8	36.6	128	22	21.20	8.495	0.464	1.43	0.16	68	GL
11	10	45.7	146	22	21.27	12.207	0.355	1.15	0.04	189	#
12	13	59.4	200	24	22.15	11.690	0.278	1.08	0.05	257	SP
13	14	64.0	174	24	22.69	9.879	0.316	1.07	0.04	234	SP
14	10	45.7	153	24	22.87	9.673	0.445	1.12	0.04	182	SP
15	8	36.6	128	24	23.04	7.060	0.558	1.28	0.16	76	GL
16	14	64.0	209	26	24.41	10.706	0.544	1.09	0.08	327	SP
17	12	54.8	179	26	24.59	7.560	0.489	1.07	0.04	257	SP
18	16	73.1	231	26	24.31	11.810	0.517	1.00	0.04	429	SP
19	16	73.1	235	28	26.04	8.995	0.442	1.07	0.05	450	SP
20	18	77.5	254	28	26.00	10.073	0.514	1.03	0.06	563	SP
21	10	45.7	143	20	19.65	13.856	0.354	1.51	0.27	119	SC
22	12	54.8	168	22	21.19	14.042	0.320	1.37	0.16	161	SC
23	13	59.4	178	22	21.10	14.312	0.233	1.37	0.20	191	SC
24	14	64.0	193	24	22.50	14.413	0.223	1.22	0.07	290	SC
25	9	41.1	144	24	22.81	10.788	0.905	1.28	0.14	148	GL
26	14	64.0	216	25	23.23	12.397	0.507	1.12	0.07	360	SP
27	8	36.6	112	18	17.74	13.239	0.410	1.74	0.46	45	GL/SC
28	9	41.1	132	20	19.29	12.942	0.610	1.44	0.29	105	#
29	11	50.3	154	20	19.68	14.182	0.284	1.23	0.17	231	SC
30	9	41.1	134	21	20.34	13.588	0.376	1.53	0.28	86	#
31	11	50.3	161	22	21.32	14.063	0.391	1.34	0.11	188	SC
32	13	59.4	182	23	21.86	14.178	0.229	1.19	0.10	281	SC

Table 2. Results of the tests with mixture Ar + 25% He and 1.0 mm diameter wire.

N^O	WS [m/min]	TS [cm/min]	I_a [A]	U_{ref} [V]	U_a [V]	l [mm]	SD	D_{drop} [mm]	SD	F [Hz]	Modtrans
1	12.0	54.8	137	20	19.51	13.777	0.274	1.23	0.26	228	SC
2	8.0	36.6	112	20	19.38	10.091	1.996	1.78	0.39	35	GL
3	10.0	45.7	141	22	21.30	12.630	0.687	1.27	0.16	250	#
4	8.0	36.6	93	22	21.43	9.430	1.149	1.75	0.19	35	GL
5	7.0	32.0	92	22	21.32	10.776	0.983	1.63	0.21	60	GL
6	12.0	54.8	164	24	22.90	11.471	0.553	1.10	0.03	237	SP
7	10.0	45.7	144	26	24.94	9.051	0.682	1.24	0.12	128	GL
8	12.0	54.8	166	26	24.84	8.852	0.589	1.20	0.17	196	#
9	14.0	64.0	182	26	24.66	10.094	0.874	1.02	0.06	346	SP
10	16.0	73.1	187	26	24.58	10.528	0.725	1.09	0.04	243	SP
11	16.0	73.1	208	28	26.35	9.839	0.894	1.03	0.06	400	SP
12	14.0	64.0	197	28	26.45	8.964	0.924	1.04	0.05	321	SP
13	18.0	77.5	221	28	26.28	9.650	0.562	0.99	0.07	409	SP
14	12.0	54.8	156	28	26.64	5.388	0.562	1.18	0.04	200	GL
15	6.0	27.4	58	20	19.85	11.382	1.190	2.91	0.44	8	GL/SC
16	12.0	54.8	147	22	21.19	13.149	0.453	1.28	0.06	130	#
17	14.0	64.0	174	24	22.77	11.883	0.544	1.08	0.03	225	SP
18	10.0	45.7	134	24	23.01	11.970	0.797	1.18	0.04	145	GL

Table 3. Results of the tests with argon gas and 1.2 mm diameter wire.

| N^O	WS [m/min]	TS [cm/min]	I_a [A]	U_{ref} [V]	U_a [V]	l [mm]	SD	D_{drop} [mm]	SD	F [Hz]	Modtrans
1	8.0	36.6	175	20	19.19	13.433	0.317	1.40	0.17	113	SC
2	6.0	27.4	120	20	19.52	12.142	1.051	1.86	0.36	49	#
3	5.0	22.9	109	20	19.54	9.767	0.751	1.83	0.31	31	GL
4	8.0	36.6	175	22	21.03	13.354	0.593	1.37	0.10	144	SC
5	6.0	27.4	130	22	21.40	9.086	0.504	1.47	0.26	78	GL
6	5.0	22.9	113	22	21.57	7.657	0.459	1.58	0.29	58	GL
7	8.0	36.6	178	24	22.93	8.933	0.408	1.19	0.03	165	SP
8	10.0	45.7	227	24	22.62	12.586	0.541	1.22	0.08	269	SP
9	6.0	27.4	135	24	23.13	7.083	0.574	1.36	0.30	77	GL
10	8.0	36.6	163	18	17.44	14.042	0.270	1.55	0.23	127	SC
11	6.0	27.4	129	18	17.59	12.802	0.623	2.06	0.26	32	GL/SC
12	4.0	18.1	73	18	17.84	9.804	1.130	2.48	0.30	10	GL
13	5.0	22.9	82	18	17.61	11.056	1.191	3.15	0.80	7	GL/SC
14	7.0	32.0	120	18	17.85	13.461	0.338	1.83	0.57	44	GL/SC
15	6.0	27.4	125	19	18.41	12.778	0.774	1.85	0.31	49	#
16	7.0	32.0	146	20	19.21	13.278	0.610	1.67	0.30	79	SC
17	6.0	27.4	128	21	20.10	12.213	0.853	1.65	0.22	65	GL
18	7.0	32.0	152	22	20.92	12.680	0.872	1.36	0.18	173	#
19	8.0	36.6	168	23	21.74	12.996	0.605	1.32	0.07	164	SP
20	9.0	41.1	186	23	21.71	13.935	0.464	1.37	0.02	170	SC
21	7.0	32.0	155	24	22.81	9.240	0.526	1.38	0.05	135	GL
22	9.0	41.1	197	25	23.50	11.489	0.365	1.21	0.10	225	SP
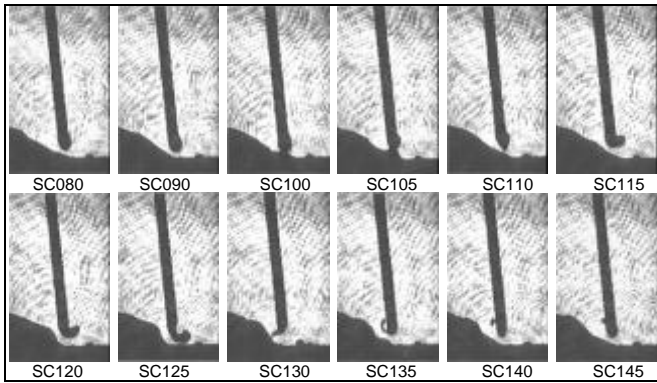
Figure 1. Figure of a short circuit transfer (test 3 of Table 1).
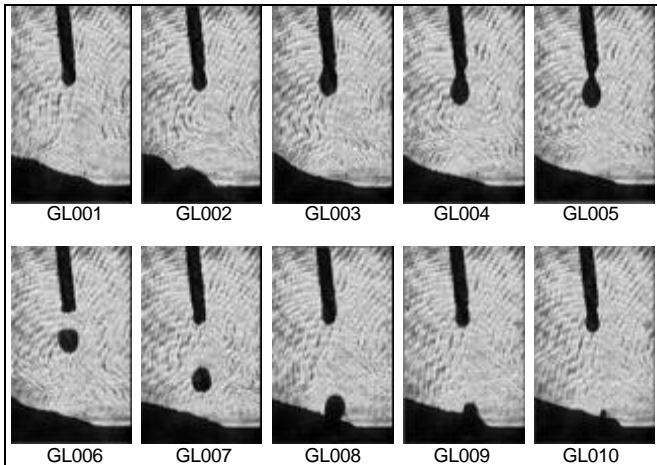

Figure 2. Photo sequence of a transfer in the globular mode (test 10 of Table 1).
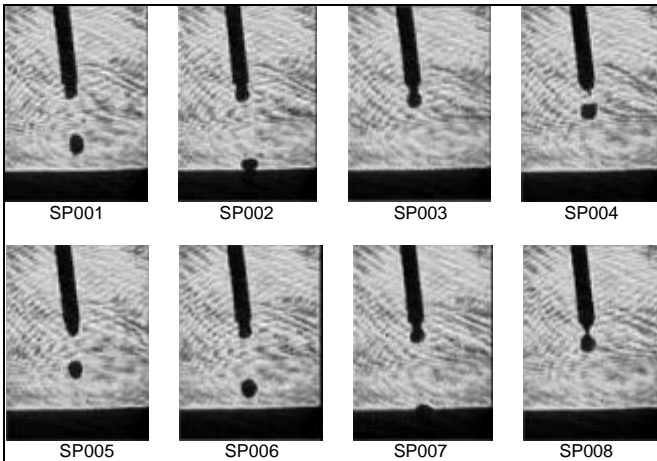

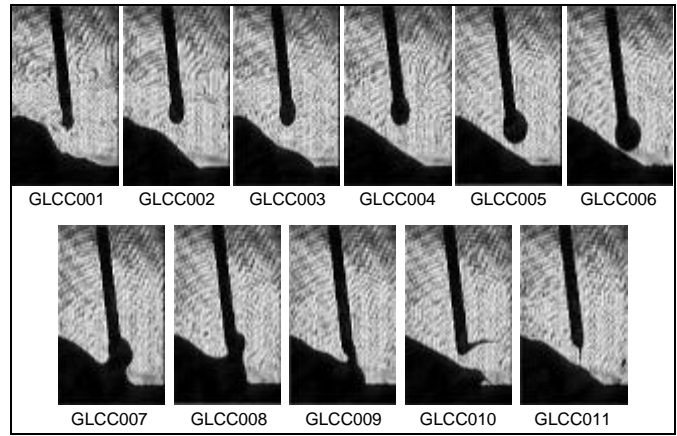Figure 3. Photo sequence of a spray transfer (test 19 of Table 1).

Figure 4. Photo sequence of transfer in the globular/short circuit mode (test 1 of Table 1).

Figures 5, 6, and 7 show the graphs of metal transfer frequency and welding average current for the tests of Tables 1, 2, and 3 which presented both globular and spray modes. For the tests with pure Ar and 1.0 mm diameter wire, the transition current was between 144 and 153 A (Figure 5). With the mixture Ar + 25% He and 1.0 mm diameter wire, this current was between 156 and 164 A (Figure 6), showing an increase compared to pure Ar. This increase is, probably, related to the change in thermal conductivity and the ionization potential of the shielding gas. For the tests with 1.2 mm wire and pure Ar, the transition current was between 155 and 168 A (Figure 7); showing that there was a growth of the current, compared to the tests with 1.0 mm wire. The increase in the transition zone current can be explained by the need of a higher current density, so that the arc may reach the necessary temperature for the occurrence of wire melting.

It is important to observe in Figures 5, 6, and 7 that it is not possible to note an abrupt increase in the frequency of the transition zone current between globular to spray mode, as is sometimes suggested in current literature (AWS, 1991). The transition zone current can be determined using the frequency increase with the welding current. This same observation was verified in the Scotti et. al. (1999) studies with stainless steel.
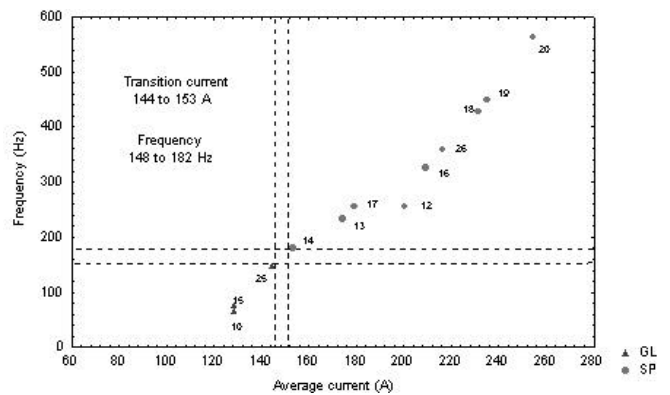

Figure 5. Average welding current against metal transfer frequency, for welding with pure Ar and 1.0 mm wire.
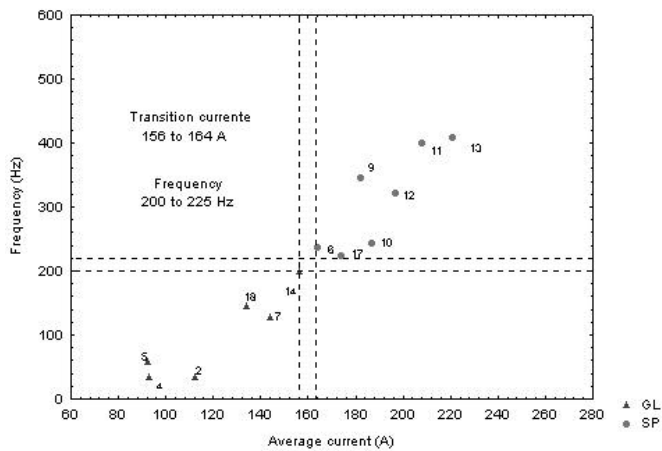
Figure 6. Average welding current against metal transfer frequency, for welding with gas mixture (Ar + 25% He) and 1.0 mm wire.
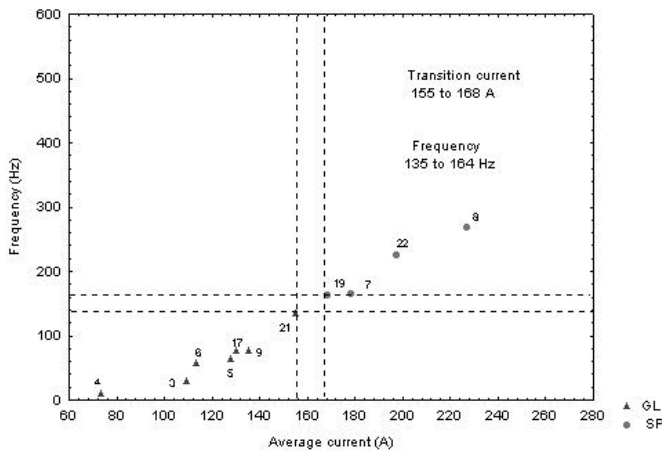

Figure 7. Average welding current against metal transfer frequency, for welding with pure Ar and 1.2 mm wire.

Figures 8, 9, and 10 show maps of the reference voltage and wire feed speed used in the tests. The regions II and I are areas in which it was impossible to accomplish tests due to burning of the contact tip and the instability of the welding process, respectively. Based on the experimental points, the limits between the regions of different modes were outlined for better visualization.

Comparing Figure 8 with Figure 9, which show the change from pure Ar to Ar + 25% He, a displacement of the globular transfer mode zone can be verified, to higher wire feed speeds as well as welding average voltage. In the spray mode it was observed only a displacement of the region to higher wire feed speed without modifying the welding average voltage. These differences between the results are probably related to the fact that the ionization potential and thermal conductivity are higher in the mixture Ar + 25% He.

Comparing Figure 8 with Figure 10 which shows a change from 1.0 mm diameter to 1.2 mm diameter in the wire, a sensible increase in the globular transfer mode zone can be verified, that is to say, it reaches a higher wire feed speed zone (welding current) within the transfer map. In the other transfer modes, the changes of the regions were not very significant.
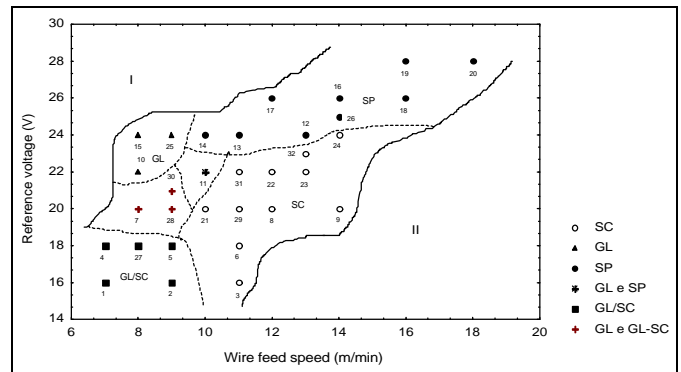

Figure 8. Map of the reference voltage and wire feed speed using 1.0 mm wire and pure Ar.
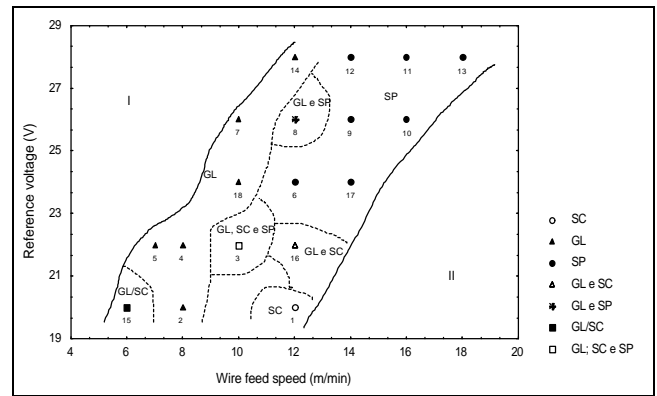

Figure 9. Map of the reference voltage and wire feed speed using 1.0 mm wire and gas mixture (Ar + 25% He).
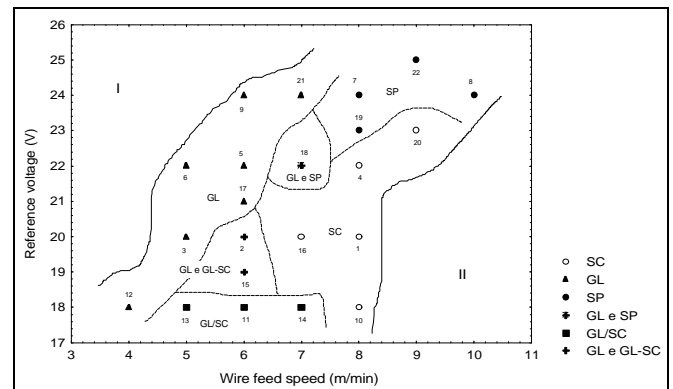

Figure 10. Map of the reference voltage and wire feed speed using 1.2 mm wire and pure Ar.

To predict the wire feed speed and, consequently, the wire consumption, the melting rate equation (Equation 1) was used. The α and β constants were determined using the data presented in Tables 1, 2, and 3, and a statistical program (nonlinear regression – Quasi-Newton estimation method). The values related to α and β are presented in Table 4.

It can be observed that for the 1.2 mm wire and argon gas tests, the β value found has a negative signal. This is probably due to the low electric resistivity of aluminum. However, the minimum value expected is zero, and not a negative value. Scotti (1991), mentioning other authors, wrote about the precautions that are necessary in the interpretation of the coefficients achieved through a regression: "occasionally the analyst experiences an apparent contradiction of

intuition or theory when one or more of the regression coefficients seems to have the "wrong" sign. Reasons for this can be: the small range of the regressions, no inclusion of an important factor in the model and the presence of multicollinearity. Due to this observation, the β value equal zero was adopted for the case of negative value.

Table 4. Values of the a and b constants.

Gas type	Wire diameter [mm]	α [kg.h^{-1}.A^{-1}]	β [kg.m^{-1}.h^{-1}.A^{-2}]
Ar	1.0	3.46×10^{-2}	4.27×10^{-4}
Ar + 25%He	1.0	3.68×10^{-2}	1.56×10^{-3}
Ar	1.2	3.61×10^{-2}	-8.79×10^{-4}

Figure 11 shows the melting rate in kg/h with the welding current. It can be observed that the test consumption with the mixture Ar + 25% He is highest, whereas with pure argon, the melting rate is practically constant for both 1.0 mm wire and 1.2 mm wire. Such fact can be explained by the higher ionization potential of the mixture Ar + 25% He, thus generating a hotter arc and higher temperatures. In the case of Ar gas the 1.2 mm wire, should theoretically present a smaller melting rate than the 1.0 mm wire for given current values, due to a smaller current density (higher diameter). However this was not significant in the results of this study.
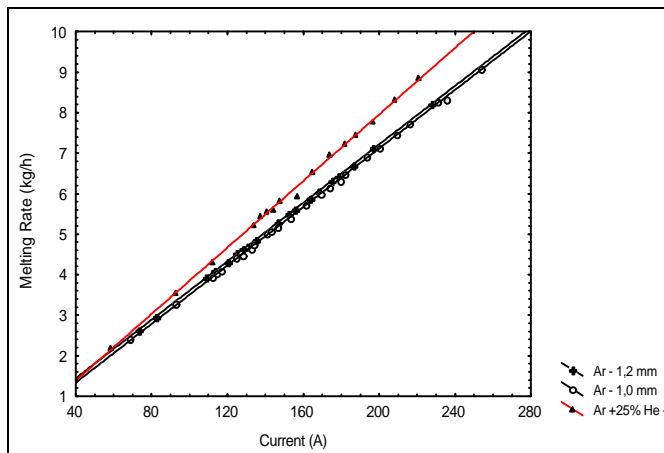

Figure 11. Graph of the melting rate against current.

Conclusions

Four major metal transfer modes were found in GMAW aluminum welding. They are: short circuit, globular, spray, and globular/short circuit.

In the spray transfer mode it was not possible to obtain drops with average diameter smaller than the wire diameter, for the test conditions analyzed in this study.

Regarding the change of the shielding gas from pure argon to argon with 25% of helium, the following changes can be observed: the globular transfer zone increased with the wire feed speed (welding current), and with the welding average voltage. In the spray mode, only a shift of the region to higher wire feed speed (welding current) occurred without increase in the welding average voltage. Another factor observed was the elevation in the globular/spray transition current and frequency.

Increasing the wire diameter from 1.0 mm to 1.2 mm, an enlargement in the region of the globular transfer mode occurred. Other factors also observed were an increase of the globular/spray transition current, and a decrease in the transition frequency.

The melting rate increases significantly when changing from Ar to Ar + 25%He. The effect of wire diameter on the melting rate is less significant.

Acknowledgments

References

AWS, 1991, Welding Handbook, Welding Processes, American Welding Society, vol. 2, 8. Ed., USA.

Figueiredo, K.M. & Ferraresi, V.A., 2000, "Influência do tipo de gás de proteção nos modos de transferência metálica na soldagem MIG de alumínio", In: Annals of the XXVI Congresso Nacional de Soldagem, September 03 to 06, Curitiba, Paraná, Brazil [in portuguese].

Lesnewich, A., 1958, "Control of Melting Rate and Metal Transfer in Gas Shielded Metal-Arc Welding: Part I – Control of Electrode Melting Rate", Welding Journal, August, pp. 343s-353s.

Norrish, J. & Richardson, I.F., 1988, "Back to Basics: Metal Transfer Mechanisms", Welding & Metal Fabrication, jan.-feb., pp. 17-22.

Quites, A.M. & Dutra, J.C., 1979, "Tecnologia da Soldagem a Arco Voltaico", EDEME, Florianópolis, Santa Catarina, Brazil [in portuguese].

Scotti, A., Clark, D.E. & Kenney, K., 1999, "Mapeamento da Transferência Metálica em MIG com Aço Inoxidável", In: Annals of the VI Seminário Brasileiro do Aço Inoxidável, May 04 and 05, São Paulo, Brazil [in portuguese].

Scotti, A., 1991, "Process Modeling to Establish Control Algorithms for Automated GMAW", PhD Thesis, Cranfield Institute of Technology, School of Industrial and Manufacturing Science, September.

Vilarinho, L.O., 2000, "Desenvolvimento e Avaliação de um Algorítimo Alternativo para Soldagem MIG Sinérgica de Alumínio", MSc Dissertation, Faculdade de Engenharia de Uberlândia, Universidade Federal de Uberlândia, February 01, Uberlândia, Minas Gerais, Brazil [in portuguese]